Available online at www.elixirpublishers.com (Elixir International Journal)

Renewable Energy Engineering

Elixir Renewable Energy Engg. 67 (2014) 21581-21586

ISSN: 2229-712X

Modeling of Offshore Wind and Tidal Current Turbines for Stability Analysis

Hamed H. H. Aly and M. E. El-Hawary

Department of Electrical and Computer Engineering, Dalhousie University, Halifax, NS, B3H 4R2, Canada.

ARTICLE INFO

Article history:

Received: 19 April 2013;

Received in revised form:

25 November 2013;

Accepted: 29 November 2013;

Keywords

Offshore wind,

Tidal current power,

Direct drive permanent magnet synchronous generator (DDPMSG),

Doubly fed induction generator (DFIG),

Squirrel cage induction generator (SCIG).

ABSTRACT

Offshore wind and tidal current are of the most common energy resources for generating electricity in the near future because of the oil problems (crises and pollution). The dynamic model of the offshore wind and tidal current are very important topic for dealing with these renewable energies. This paper describes the overall dynamic models of tidal current turbine using three different types of generators (doubly fed induction generator (DFIG), squirrel cage induction generator (SCIG) and direct drive permanent magnet synchronous generator (DDPMSG)). The state space for all types of the generators of these two types of turbines are concluded. All models are validated using a common property of the generator for the validation.

Introduction

Wind energy is the energy produced from the simple air in motion and this motion is caused by the uneven heating of the earth's surface by the sun. The air over the sea absorbs the heats faster than the land and so the air moves from the sea to the land causing the wind but in the night the air motion is changed from the land to the sea because the air over the sea cools faster than the air over the land. This wind is hardly predictable source of energy. Tidal current turbines extract electric energy from the water. Tidal currents are fluctuating, intermittent but a predictable source of energy. Its use is very effective as it relies on the same technologies used in wind turbines but it is still under development and requires more research. There are two tide types; spring tide which happens when the moon and the sun are on the same line and neap tide which happens when the moon and the sun are at right angles and so they pull water at the sea in different directions. The electrical-side layout and modeling approaches used in tidal in-stream systems are similar to those used for wind and offshore wind systems. The speed of water currents is lower than wind speed, while the water density is higher than the air density and as a result wind turbines operate at higher rotational speeds and lower torque than tidal in-stream turbines which operate at lower rotational speed and high torque [1-5].

The easier predictability of the tidal in-stream energy resource makes it easier to integrate in an electric power grid. Recognizing that future ocean energy resources are available far from load centers and in areas with limited grid capacity will result in challenges and technical limitations. With the growing penetration of tidal current energy into the electric power grid system, it is very important to study the impact of tidal current turbines on the stability of the power system grid and to do that we should model the overall system. The model of the ocean energy system consists of three stages. The first stage contains the fluid mechanical process. The second stage consists of the mechanical conversion and depends on the relative motion between bodies. This motion may be mechanical transmission and then using mechanical gears or may be depending on the hydraulic pumps and hydraulic motors. The third stage consists of the electromechanical conversion to the electrical grid [4-9].

Offshor wind and TIDAL CURRENT MODEL using IG

This section describes the dynamic model of the offshore wind and tidal current turbine system, DFIG, SCIG, the converter and the controllers.

The speed signal resource model for the tidal current and offshore wind

The tidal current speed may be expressed as a function of the spring tide speed, neap tide speed and tides coefficient. Paper (10) proposed different algorithm models for the tidal current speed.

The Wind Speed Signals Model (v_w) consists of four components related to the mean wind speed (v_{mw}), the wind speed ramp (v_{rw}) (which is considered as the steady increase in the mean wind speed), the wind speed gust (v_{gw}), and the turbulence (v_{tw}).

$$v_w = v_{mw} + v_{gw} + v_{rw} + v_{tw}$$

The mean wind speed is a constant; a simple ramp function will be used for ramp component (characterized by the amplitude of the wind speed ramp (A_r (m/s)), the starting time (T_{sr}), and the ending time (T_{er})). The wind speed gust component is characterized by the amplitude of the wind speed gust (A_g (m/s)), the starting time (T_{sg}), and the ending time (T_{eg}). The wind speed gust may be expressed as a sinusoidal function.

The most used models are given by:

$$v_{gw} = A_g(1-\cos(2\Pi(t/D_g - T_{sg}/D_g))) \qquad T_{sg} \le t \le T_{eg}$$

$$v_{gw} = 0 \qquad t < T_{sg} \text{ or } t > T_{eg}$$

$$D_g = T_{eg} - T_{sg}$$

A triangular wave is used to represent the turbulence function which has adjustable frequency and amplitude [11].

Tele:

E-mail addresses: Hawary@yahoo.co.in

The rotor model

For the offshore wind the rotor model represents the conversion of kinetic energy to mechanical energy. The wind turbine is characterized by C_p (wind power coefficient), λ (tip speed ratio), and β (pitch angle). $\lambda = \omega_t R/v_w$, where R is the blade length in m, v_w is the wind speed in m/s, and ω_t is the wind turbine rotational speed in rad/sec. C_P-λ-β curves are manufacturer-dependent but there is an approximate relation expressed as

$$C_p = \frac{1}{2\left(\frac{RC_f}{\lambda} - 0.026\,\beta - 2\right)e^{-0.295\frac{RC_f}{\lambda}}},$$

C_f is the wind turbine blade design constant.

The rotor model may be represented by using the equation of the power extracted from the wind (P_w = 0.5((□ R□↑2 C↓p v↓w↑3), or the mechanical torque applied to the turbine ( ), v_m is the turbine speed at hub height upstream the rotor, ρ is the density of the air [11].

For the tidal current turbines the rotor model may be represented by using the equation of the power extracted from the wind (P_w = 0.5((□ R□↑2 C↓p v↓w↑3),

The power (P_{ts}) may be found using: $P_{ts} = ½\ \rho A(V_{tide})^3$. The turbine harnesses a fraction of this power, hence the power output may be expressed as: $P_t = ½\ \rho C_p A(V_{tide})^3$. The power output is proportional to the cube of the velocity. The velocity at the bottom of the channel is lower than at the water column above seabed. The mechanical torque applied to the turbine (T_m) can be expressed as [4-9]:

The shaft system for tidal current and offshore turbines may be represented by a two mass system one for the turbine and the other for the generator as shown:

$$2H_t \frac{d\omega_t}{dt} = T_t - K_s(\Theta_r - \Theta_t) - D_s(\omega_r - \omega_t) \quad (2)$$

$$2H_g \frac{d\omega_r}{dt} = T_e - K_s(\Theta_r - \Theta_t) - D_s(\omega_r - \omega_t) \quad (3)$$

$$\Theta_{tr} = \Theta_r - \Theta_t \quad (4)$$

$$\frac{d\Theta\Theta tr}{dt} = \omega_r - \omega_t \quad (5)$$

There is a ratio for the torsion angles, damping and stiffness that need to be considered when one adds a gear box as all above calculations must be referred to the generator side and calculated as : $a = \frac{\omega_r}{\omega_t}$, $\omega_r^{(t)} = \frac{\omega_r^{(g)}}{a}$, $\Theta_t^{(t)} = \frac{\Theta_t^{(g)}}{a}$, $K_s^{(t)} = a^2 K_s^{(g)}$, $D_m^{(t)} = a^2 D_m^{(g)}$. The same model used for the offshore wind is used for tidal in-stream turbines; however, there is a number of differences in the design and operation of marine turbines due to the changes in force loadings, immersion depth, and different stall characteristics. Since the extracted power from the tidal currents is proportional to the area and the cube of the velocity, hence narrow channels is preferred for tidal turbines to extract higher power as the velocity is higher.

Dynamic model of DFIG

The DFIG model is developed using a synchronously rotating d-q reference frame with the direct-axis oriented along the stator flux position. The reference frame rotates at the same speed as the stator voltage. The stator and rotor active and reactive power are given by [4-10]:

$P_s = 3/2(v_{ds}\ i_{ds} + v_{qs}\ i_{qs})$, $P_r = 3/2(v_{dr}\ i_{dr} + v_{qr}\ i_{qr})$ (6)

$P_g = P_s + P_r$ (7)

$Q_s = 3/2(v_{qs}\ i_{ds} - v_{ds}\ i_{qs})$, $Q_r = 3/2(v_{qr}\ i_{dr} - v_{dr}\ i_{qr})$ (8)

The model of the DFIG can be described as:

$$v_{ds} = -R_s\ i_{ds} - \omega_s\ \psi_{qs} + \frac{d}{dt}\psi_{ds} \quad (9)$$

$$v_{qs} = -R_s\ i_{qs} + \omega_s\ \psi_{ds} + \frac{d}{dt}\psi_{qs} \quad (10)$$

$$v_{dr} = -R_r\ i_{dr} - s\ \omega_s\ \psi_{qr} + \frac{d}{dt}\psi_{dr} \quad (11)$$

$$v_{qr} = -R_r\ i_{qr} + s\ \omega_s\ \psi_{dr} + \frac{d}{dt}\psi_{qr} \quad (12)$$

$\Psi_{ds} = -L_{ss}\ i_{ds} - L_m\ i_{dr}$, $\Psi_{qs} = -L_{ss}\ i_{qs} - L_m\ i_{qr}$ (13)

$\Psi_{dr} = -L_{rr}\ i_{dr} - L_m\ i_{ds}$, $\Psi_{qr} = -L_{rr}\ i_{qr} - L_m\ i_{qs}$ (14)

$s = (\omega_s - \omega_r)/\omega_s$ (15)

$\frac{d\omega_r}{dt} = -\omega_s \frac{ds}{dt}$ (16)

Where, $L_{ss} = L_s + L_m$, $L_{rr} = L_r + L_m$, L_s, L_r and L_m are the stator leakage, rotor leakage and mutual inductances, respectively. The previous model may be reduced by neglecting stator transients and is described as follows:

$$v_{ds} = -R_s\ i_{ds} + X'\ i_{qs} + e_d \quad (17)$$

$$v_{qs} = -R_s\ i_{qs} - X'\ i_{ds} + e_q \quad (18)$$

$$\frac{de_d}{dt} = -\frac{1}{T_o}\left(e_d + (X - X□)i_{qs}\right) + s\ \omega_s\ e_q - \omega_s \frac{L_m}{L_{rr}} v_{qr} \quad (19)$$

$$\frac{de_q}{dt} = -\frac{1}{T_o}\left(e_q - (X - X□)i_{ds}\right) - s\ \omega_s\ e_d + \omega_s \frac{L_m}{L_{rr}} v_{dr} \quad (20)$$

The components of the voltage behind the transient (the internal voltage components of the induction generator) are $e_d = -\frac{\omega_s L_m}{L_{rr}}\psi_{qr}$ and $e_q = \frac{\omega_s L_m}{L_{rr}}\psi_{dr}$. The stator reactance $X = \omega_s L_{ss} = X_s + X_m$, and the stator transient reactance $X' = \omega_s (L_{ss} - L_m^2/L_{rr}) = X_s + (X_r\ X_m)/(X_r + X_m)$. The transient open circuit time constant is $T_o = L_{rr}/R_r = (L_r + L_m)/R_r$, and the electrical torque is $T_e = (i_{ds}i_{qr} - i_{qs}i_{dr})X_m/\omega_s$. Figure (1) shows d and q – axis equivalent circuit of DFIG.

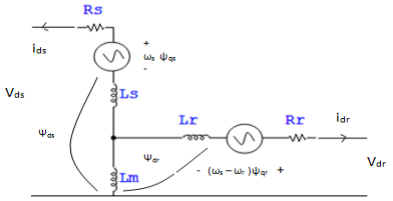

d – axis equivalent circuit of DFIG

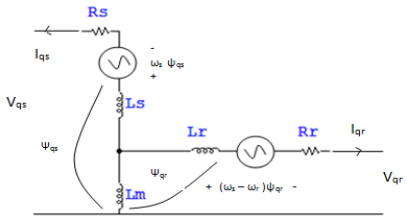

q – axis equivalent circuit of DFIG

Figure (1) d and q – axis equivalent circuit of DFIG

Dynamic model of (Squirrel Cage Induction Generator) SCIG

In the SCIG the rotor is short circuited and so, the stator voltages are the same as the DFIG:

$$v_{ds} = -R_s\ i_{ds} + \omega_s\ \psi_{qs} - \frac{d}{dt}\psi_{ds}$$

$$v_{qs} = -R_s\ i_{qs} - \omega_s\ \psi_{ds} - \frac{d}{dt}\psi_{qs}$$

$$0 = -R_r\ i_{dr} + s\ \omega_s\ \psi_{qr} - \frac{d}{dt}\psi_{dr}$$

$$0 = -R_r\ i_{qr} - s\ \omega_s\ \psi_{dr} - \frac{d}{dt}\psi_{qr}$$

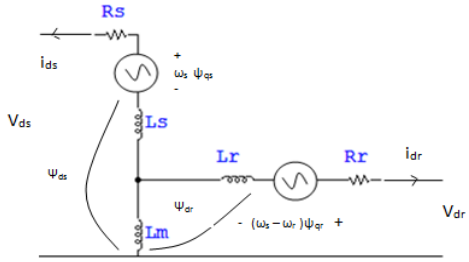

d – axis equivalent circuit of SCIG

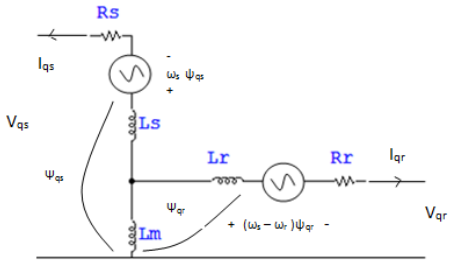

q – axis equivalent circuit of SCIG

Figure (2) d and q – axis equivalent circuit of FSIG

$P_r = 0$; $Q_r = 0$

In the SCIG there are capacitors to provide the induction generator magnetizing current and for compensation. Figure (2) d and q – axis equivalent circuit of FSIG.

The pitch controller model

The pitch controller is used to adjust the tidal current turbine to achieve a high speed magnitude. This may be represented by a PI controller with a transfer function $K_{pt} + \frac{K_{it}}{S}$ shown in Figure (3).

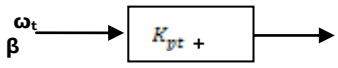

Figure (3) Pitch angle control block

$$\beta = (K_{pt} + \frac{K_{it}}{S})\omega_t \quad (21)$$

$$\frac{d\beta}{dt} = K_{pt}\frac{d\omega t}{dt} + K_{it}\,\omega_t \quad (22)$$

The converter model

A converter feeds or takes power from the rotor circuit and gives a variable speed (a partial scale power converter used). The rotor side of the DFIG is connected to the grid via a back to back converter. The converter at the side connected to the grid is called the supply side converter (SSC) or grid side converter (GSC) while the converter connected to the rotor is the rotor side converter (RSC). The RSC operates in the stator flux reference frame. The direct axis component of the rotor current acts in the same way as the field current as in the synchronous generator and thus controls the reactive power change. The quadrature component of the rotor current is used to control the speed by controlling the torque and the active power change. Thus the RSC governs both the stator-side active and reactive powers independently. The GSC operates in the stator voltage reference frame. The *d*-axis current of the GSC controls the DC link voltage to a constant level, and the *q*-axis current is used for reactive power control. The GSC is used to supply or draw power from the grid according to the speed of the machine. If the speed is higher than synchronous speed it supplies power, otherwise it draws power from the grid but its main objective is to keep the dc-link voltage constant regardless of the magnitude and direction of the rotor power

The back to back converter using a DC link is shown in Figure (4). The balanced power equation is given by [13, 14]:

$$P_r = P_g + P_{DC} \quad (23)$$

$$P_{DC} = v_{DC} i_{DC} = -C v_{DC} \frac{dv_{DC}}{dt}, \quad P_q = v_{Dq} i_{Dq} + v_{Qq} i_{Qq} \quad (24)$$

$$C v_{DC} \frac{dv_{DC}}{dt} = v_{Dg} i_{Dg} + v_{Qg} i_{Qg} - v_{dr}\ i_{dr} - v_{qr}\ i_{qr} \quad (25)$$

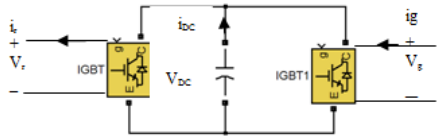

Figure (4) Back to back converter

Rotor side converter controller model

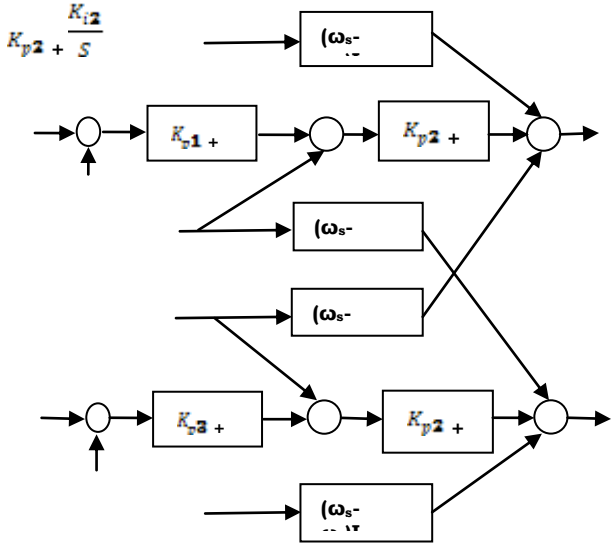

Figure (5) Generator side converter controller

The rotor side converter controller used here is represented by four states ($\dot{x}_1$, $\dot{x}_2$, $\dot{x}_3$ and $\dot{x}_4$), $\dot{x}_1$ is related to the difference between the generated power of the stator and the reference power that is required at a certain time, $\dot{x}_2$ is related to the difference between the quadrature axis generator rotor current and the reference current that is required at a certain time, $\dot{x}_3$ is related to the difference between the stator terminal voltage and the reference voltage that is required at a certain time, and $\dot{x}_4$ is related to the difference between the direct axis generator rotor current and the reference current that is required at a certain time [13, 14]. Figure (5) shows the rotor side converter controller. This is described by equations (26-34).

$$\dot{x}_1 = P_{ref} - P_s \quad (26)$$

$$\dot{x}_1 = -K_{i1}/K_{p1} x_1 + 1/K_{p1}\, i_{qr\_ref} \quad (27)$$

$$\dot{x}_2 = i_{qr\_ref} - i_{qr} \quad (28)$$

$$\dot{x}_2 = K_{p1}\dot{x}_1 + K_{i1} x_1 - i_{qr} \quad (29)$$

$$\dot{x}_2 = -K_{i2}/K_{p2} x_2 + 1/K_{p2}\, v_{qr} - \omega_s L_m/K_{p2}\, i_{ds} - \omega_s L_{rr}/K_{p2}\, i_{dr} + (L_m/K_{p2})\, i_{ds}\omega_r + (L_{rr}/K_{p2}) i_{dr}\omega_r \quad (30)$$

$$\dot{x}_3 = v_{s\_ref} - v_s \quad (31)$$

$$\dot{x}_3 = -K_{i3}/K_{p3} x_3 + 1/K_{p3}\, i_{dr\_ref} \quad (32)$$

$$\dot{x}_4 = i_{dr\_ref} - i_{dr} \quad (33)$$

$$\dot{x}_4 = -K_{i2}/K_{p2}\, x_4 + 1/K_{p2}\, v_{dr} - \omega_s L_m/K_{p2}\, i_{qs} - \omega_s L_{rr}/K_{p2}\, i_{qr} + (L_m/K_{p2})\, i_{qs}\omega_r + (L_{rr}/K_{p2})\, i_{qr}\omega_r \quad (34)$$

Grid side converter controller model

The grid side converter controller used here is represented by four states ($\dot{x}_5$, $\dot{x}_6$, $\dot{x}_7$ and $\dot{x}_8$), x_5 is related to the difference between the DC voltage and the reference DC voltage required at a certain time, x_6 related to the difference between the grid terminal voltage and the reference terminal voltage required at a certain time, x_6 is a combination of x_5 and direct axis grid current and x_8 is a combination of x_6 and quadrature axis grid current as shown in equations (35-40). Figure (6) shows the grid side converter controller.

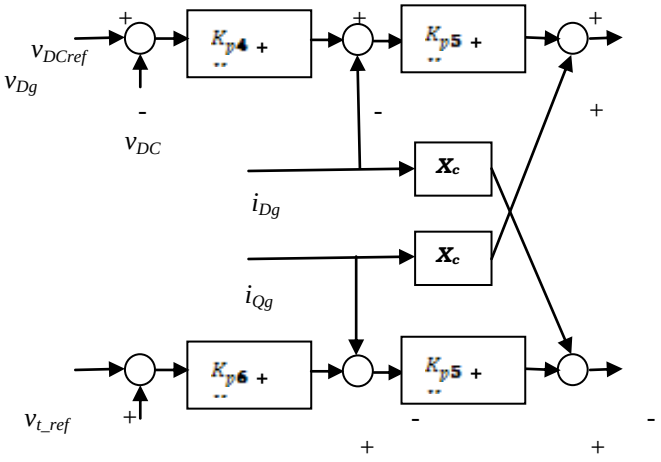

Figure (6) Grid side converter controller

$$\dot{x}_5 = v_{DC\_ref} - v_{DC} \quad (35)$$

$$\dot{x}_6 = K_{p4}\dot{x}_5 + K_{i4}x_5 - i_{Dq} \quad (36)$$

$$\dot{x}_7 = v_{t\_ref} - v_t \quad (37)$$

$$\dot{x}_8 = K_{p6}\dot{x}_7 + K_{i6}x_7 - i_{Qq} \quad (38)$$

$$v_{Dq} = K_{p5}\dot{x}_6 + K_{i5}x_6 + X_c i_{Qq} \quad (39)$$

$$v_{Qq} = K_{p5}\dot{x}_8 + K_{i5}x_8 - X_c i_{Dq} \quad (40)$$

TIDAL currnt turbine MODEL using DDPMSG

In this section we review the dynamic model of the direct drive permanent magnet synchronous generator, the converter and the proposed controllers.

The dynamic modeling of the DDPMSG

The DDPMSG can be modeled as the following [3, 13]:

$$v_{ds} = -R_s \times i_{ds} - \omega_s \times \psi_{qs} + \frac{d}{dt}\psi_{ds} \quad (41)$$

$$v_{qs} = -R_s \times i_{qs} + \omega_s \times \psi_{ds} + \frac{d}{dt}\psi_{qs} \quad (42)$$

The flux linkages and the torque can be expressed as:

$$\Psi_{ds} = -L_d \times i_{ds} + \psi_f \quad (43)$$

$$\Psi_{qs} = -L_q \times i_{qs} \quad (44)$$

$$T_e = (3/2)p\, i_{qs}((L_d - L_q)\, i_{ds} + \psi_f) \quad (45)$$

L_d, and L_q are the direct and quadrature inductances of the stator. Ψ_f is the excitation field linkage, and p is the number of pair poles. Figure (7) shows the d-q axis component of the DDPMSG. In this paper for simplicity we will assume that $L_d = L_q = L_s$, and so the generator model can be rewritten in a state space representation as:

$$L_s \frac{d}{dt} i_{ds} = -v_{ds} - R_s \times i_{ds} + L_s \times \omega_s \times i_{qs} \quad (46)$$

$$L_s \frac{d}{dt} i_{qs} = -v_{qs} - R_s \times i_{qs} - L_s \times \omega_s \times i_{ds} + \omega \times \psi_f \quad (47)$$

The converters models used for the DFIG are the same converters that used for the DDPMSG keeping in mind that a full scale power converter is used.

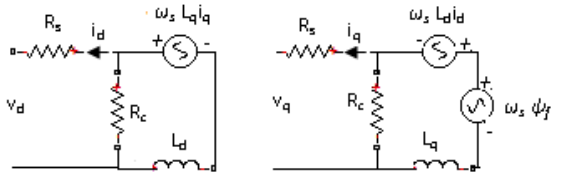

Figure (7) d-q axis component of PMSG

The generator side converter controller model for DDPMSG

The generator side converter controller used here is represented by two states only (x_1, and x_2), x_1 related to the difference between the generated power and the reference power that required at a certain time and x_2 related to the difference between the direct axis generator current and the reference current that required at a certain time [13-15]. Figure (8) shows the generator side converter controller described by:

$$\dot{x}_1 = P_s - P_{ref} \quad (48)$$

$$\dot{x}_2 = i_{ds} - i_{ds\_ref} \quad (49)$$

$$v_{qs} = K_{p1}\dot{x}_1 + K_{i1}x_1 - L_s w i_{ds} \quad (50)$$

$$v_{ds} = K_{p2}\dot{x}_2 + K_{i2}x_2 + L_s w i_{qs} \quad (51)$$

Where: K_{p1}, K_{p2}, represent the proportional controller constants and K_{i1}, K_{i2} represent the integral controller constants for the generator side converter controller.

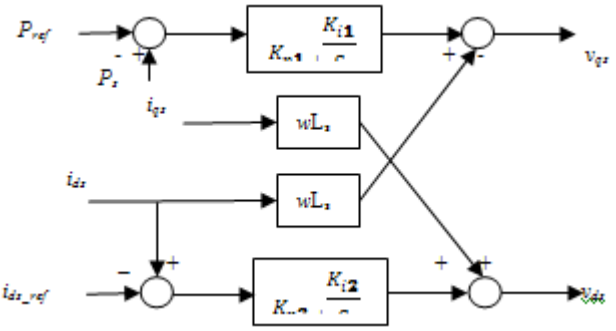

Figure (8) Generator side converter controller for DDPMSG

Grid side converter controller model for DDPMSG

The grid side converter controller used here is represented by four states (x_3, x_4, x_5, x_6), x_3 related to the difference between the DC voltage and the reference DC voltage that required at a certain time, x_5 related to the difference between the terminal voltage and the reference terminal voltage that required at a certain time, x_4 is a combination of x_3 and direct axis grid current and x_6 is a combination of x_4 and quadrature axis grid current. Figure (9) shows the grid side converter controller.

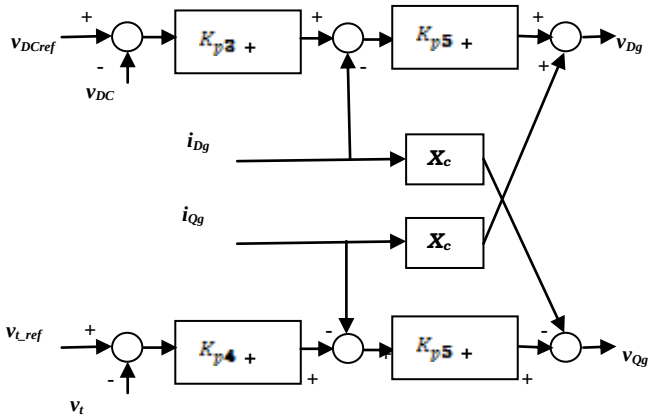

Figure (9) Grid side converter controller for DDPMSG

$$\dot{x}_3 = v_{sDC\_ref} - v_{DC} \quad (52)$$

$$\dot{x}_4 = K_{p3}\dot{x}_3 + K_{i3}x_3 - i_{Dq} \quad (53)$$

$$\dot{x}_5 = v_{t\_ref} - v_t \quad (54)$$

$$\dot{x}_6 = K_{p4}\dot{x}_4 + K_{i4}x_5 - i_{Qg} \quad (55)$$

$$v_{Dg} = K_{p5}\dot{x}_4 + K_{i5}x_4 + X_c i_{Qg} \quad (56)$$

$$v_{Qg} = K_{p5}\dot{x}_6 + K_{i5}x_6 - X_c i_{Dg} \quad (57)$$

Where: V_{DC} is the DC link voltage, i_{Dg}, i_{Qg} are the D and Q axis grid currents, v_{Dg}, v_{Qg} are the D and Q axis grid voltages, K_{p3}, K_{p4}, K_{p5} represent the proportional controller constants, X_c is the grid side smoothing reactance, and K_{i3}, K_{i4}, K_{i5} represent the integral controller constants for the grid side converter.

Validation of the models

As the value of the resistance or inductance changes the stability degree will change. In this section we will try to find the relation between the increasing or decreasing of these values and the stability degree as a way of validation for the models. Figure (10) shows the relation between different values of the rotor resistance and the eigenvalues of the changed mode in case of DFIG. Figure (11) shows the relation between different values of the stator resistance and the eigenvalues of the changed mode in case of DDPMSG. From Figures (11, 12) we conclude that as the resistance value of the rotor increase, the stability degree will increase. Figure (12) shows the relation between different values of the rotor inductance and the eigenvalues of the changed mode in case of DFIG. Figure (13) shows the relation between different values of the stator inductance and the eigenvalues of the changed mode in case of DDPMSG. From Figures (12, 13) we conclude that as the inductance value increase as the stability will decrease because of increasing the delay time.

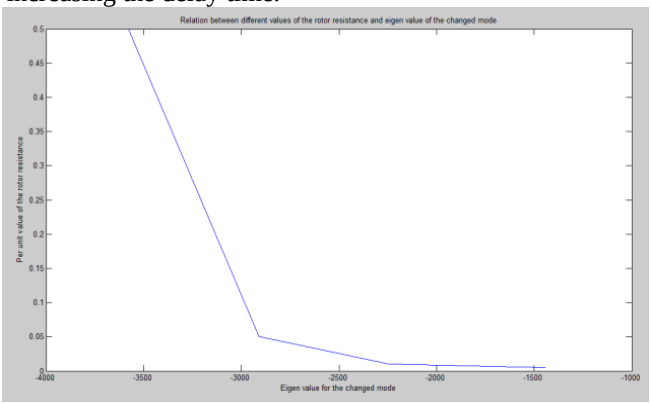

Figure (10) The relation between different values of the rotor resistance and the eigenvalues of the changed mode in case of DFIG

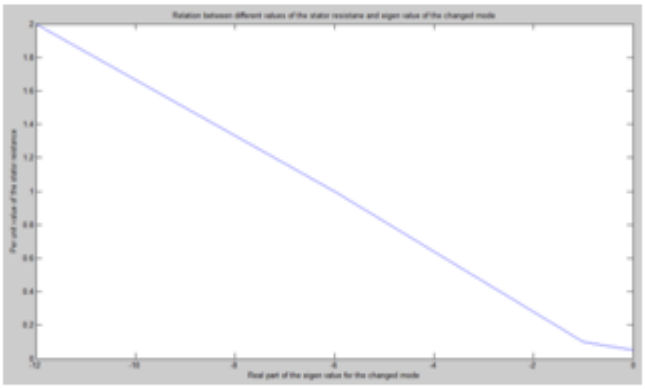

Figure (11) The relation between different values of the stator resistance and the eigenvalues of the changed mode in case of DDPMSG

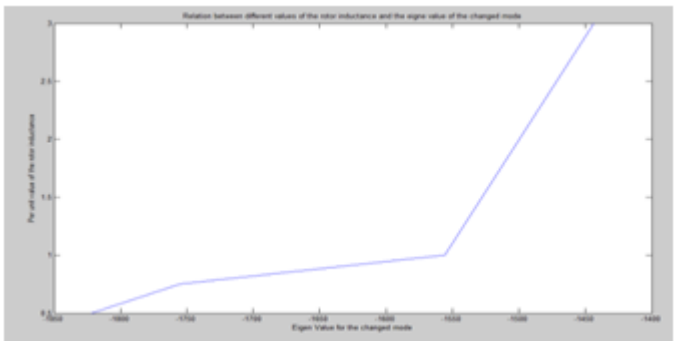

Figure (12) The relation between different values of the rotor inductance and the eigenvalues of the changed mode in case of DFIG

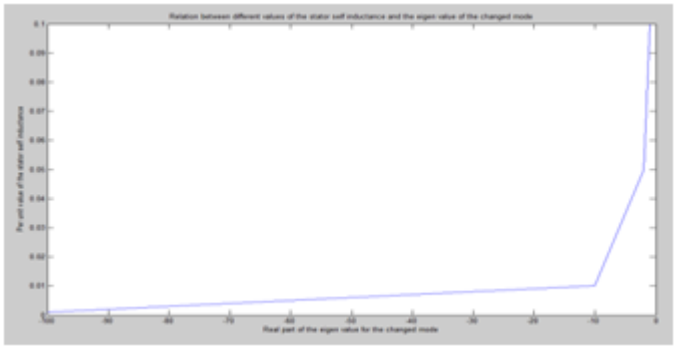

Figure (13) The relation between different values of the stator self inductance and the eigenvalues of the changed mode in case of DDPMSG.

Conclusion

The use of offshore wind and tidal current as a renewable source of energy is very effective as it relies on similar technologies. The overall dynamic system of the offshore and tidal current turbine based on three different types of generators for a single machine infinite bus system has been modeled. The converter used has been modelled. Different controllers are also models for different machines. The state space representation of the overall system is concluded. All models are validated using a common property of the machine for the validation (changing the degree of the system stability by changing of the value of the resistance and the inductance). If the resistance value of different generators increases, the stability degree will increase and if the inductance value of the machine increases, the stability degree will decrease.

References

[1]"Tidal Stream" Available online (January 2011), http://www.tidalstream.co.uk/html/background.html

[2]"Tidal Currents" Available online (April 2011), http://science.howstuffworks.com/environmental/earth/oceanography/ocean-current4.htm

[3] Hamed H. H. Aly, and M. E. El-Hawary "State of the Art for Tidal Currents Electrical Energy Resources", 24th Annual Canadian IEEE Conference on Electrical and Computer Engineering, Niagara Falls, Ontario, Canada, 2011.

[4] Hamed H. Aly, and M. E. El-Hawary "An Overview of Offshore Wind Electrical Energy Systems" 23rd Annual Canadian IEEE Conference on Electrical and Computer Engineering, Calgary, Alberta, Canada, May 2-5, 2010.

[5] Marcus V. A. Nunes, J. A. Peças Lopes, Hans Helmut, Ubiratan H. Bezerra, and Rogério G. "Influence of the Variable-Speed Wind Generators in Transient Stability Margin of the Conventional Generators Integrated in Electrical Grids" IEEE Transactions on Energy Conversion, 2004.

[6] J.G. Slootweg, H. Polinder and W.L. Kling"Dynamic Modeling of a Wind Turbine with Doubly Fed Induction Generator" IEEE Power Engineering Society Summer Meeting, 2001.
[7] Janaka B. Ekanayake, Lee Holdsworth, XueGuang Wu, and Nicholas Jenkins" Dynamic Modeling of Doubly Fed Induction Generator Wind Turbines" IEEE Transactions on Power Systems, Vol. 18, No. 2, May 2003.
[8] M.J.Khan, G. Bhuyan, A. Moshref, K. Morison, "An Assessment of Variable Characteristics of the Pacific Northwest Regions Wave and Tidal Current Power Resources, and their Interaction with Electricity Demand & Implications for Large Scale Development Scenarios for the Region," Tech. Rep. 17485-21-00 (Rep 3), Jan. 2008.
[9] Lucian Mihet-Popa, Frede Blaabjerg, and Ion Boldea," Wind Turbine Generator Modeling and Simulation Where Rotational Speed is the Controlled Variable" IEEE Transactions On Industry Applications, Vol. 58, No. 1, January/February 2004.
[10] Hamed H. H. Aly, M. E. El-Hawary. A Proposed Algorithms for Tidal in-Stream Speed Model. American Journal of Energy Engineering. Vol. 1, No. 1, 2013, pp. 1-10.
[11] Hamed H. H. Aly, M. E. El-Hawary. The Current Status of Wind and Tidal in-Stream Electric Energy Resources, American Journal of Electrical Power and Energy Systems. Vol. 2, No. 2, 2013, pp. 23-40.
[12] Yazhou Lei, Alan Mullane, Gordon Lightbody, and Robert Yacamini "Modeling of the Wind Turbine with a Doubly Fed Induction Generator for Grid Integration Studies" IEEE Transaction on Energy Conversion, Vol. 28, No. 1, March 2006.
[13] F. Wu, X.-P. Zhang, and P. Ju "Small signal stability analysis and control of the wind turbine with the direct-drive permanent magnet generator integrated to the grid" Journal of Electric Power and Engineering Research, 2009.
[14] F. Wu, X.-P. Zhang, and P. Ju "Small signal stability analysis and optimal control of a wind turbine with doubly fed induction generator" IET Journal of Generation, Transmission and Distribution, 2007.
[15] Hamed H. Aly "Forecasting, Modeling, and Control of Tidal currents Electrical Energy Systems "PhD thesis, Halifax, Canada. 2012.

Hamed H. H. Aly received the B.Sc. and M.Sc. degrees in electrical engineering with distinction, in 1999 and 2005, respectively, from Zagazig University, Egypt and the Ph.D. degree from Dalhousie University, Halifax, NS, Canada, in 2012. His research interests include Forecasting, Modeling, Control, power system quality, integration of the renewable energy into the electrical grid, Smart Grid and power system stability. He has written one textbook and more than 20 refereed articles. Dr. Aly is currently doing his postdoctoral fellowship and working as an instructor at Dalhousie University in the Faculty of Engineering.

M. E. El-Hawary (S'68–M'72–F'90) received the B.Eng. degree in electrical engineering with distinction from the University of Alexandria, Alexandria, Egypt, in 1968 and the Ph.D. degree from the University of Alberta, Edmonton, AB, Canada, in 1972. He was a Killam Memorial Fellow at the University of Alberta. He is now a Professor of electrical and computer engineering at Dalhousie University, Halifax, NS, Canada. He served on the faculty and was a Chair of the Electrical Engineering Department at Memorial University of Newfoundland for eight years. He was an Associate Professor of electrical engineering at the Federal University of Rio de Janeiro, Rio de Janeiro, Brazil, for two years and was Instructor at the University of Alexandria. He pioneered many computational and artificial intelligence solutions to problems in economic/environmental operation of power systems. He has written ten textbooks and monographs and more than 122 refereed journal articles. He has consulted and taught for more than 42 years.
Dr. El-Hawary is a Fellow of the Engineering Institute of Canada (EIC) and the Canadian Academy of Engineering (CAE).